Impurity gettering effect of atomic layer deposited aluminium oxide films on silicon wafers

A. Y. Liu, and D. Macdonald

Impurity gettering effect of atomic layer deposited aluminium oxide films on silicon wafers

A. Y. Liu and D. Macdonald
Research School of Engineering, College of Engineering and Computer Science,
The Australian National University, Canberra, ACT 2601, Australia

We present experimental evidence for the impurity gettering effect of atomic layer deposited aluminium oxide (Al_2O_3) films on silicon wafers, during typical surface passivation activation at 425 °C. Iron was used as a model impurity in silicon to study the gettering effects. Dissolved iron concentrations were determined by carrier lifetime measurements, allowing the iron loss kinetics in silicon wafers with Al_2O_3 coatings to be monitored during annealing. The redistribution of iron to the surface layers and the sub-surface regions was examined by secondary ion mass spectrometry depth profiling. The results show that the atomic layer deposited Al_2O_3 films generate a strong gettering effect, removing 50% of the iron after 30 min at 425 °C for a 160-μm thick silicon wafer. The iron reduction process is largely diffusion-limited in the initial stages. The gettering effect is caused by the accumulation of iron at the Al_2O_3/Si interface. *Published by AIP Publishing.*
[http://dx.doi.org/10.1063/1.4983380]

Atomic layer deposited (ALD) aluminium oxide (Al_2O_3) films provide excellent passivation for both moderately doped p- and n-type silicon surfaces and for heavily doped p-type surfaces, owing to their high fixed negative charge density and low interface defect density.[1–3] ALD Al_2O_3 films have therefore emerged as an important and widely adopted surface passivation technology in the past decade,[4] used in both p- and n-type silicon solar cells (for example, as demonstrated in Refs. 5 and 6).

The interaction of the ALD Al_2O_3 films with metallic impurities in the silicon bulk, however, remains unexplored. It was recently reported that plasma-enhanced chemical vapour deposited (PECVD) silicon nitride (SiN_x) films possess a strong gettering effect for bulk impurities, via a segregation gettering mechanism.[7] This was revealed by monitoring the redistribution of iron (Fe) in the SiN_x films and the silicon wafer bulk after annealing.[7] Here, we aim to examine the possible gettering effect of ALD Al_2O_3 films at a typical film activation temperature of 425 °C. ALD Al_2O_3 films generally require a post-deposition anneal between 300 and 500 °C, for several minutes to tens of minutes, in order to activate the surface passivation effect.[8] Iron is used as a model impurity to assess the gettering effect, as dissolved interstitial iron (Fe_i) in silicon can be easily and accurately quantified using lifetime based techniques.[9,10] Moreover, iron is a common efficiency-limiting impurity in silicon solar cells.[11] The gettering effect of the ALD Al_2O_3 films at 425 °C is examined by monitoring the Fe_i loss kinetics in the silicon wafer bulk via quasi-steady-state photoconductance (QSSPC) lifetime measurements and by assessing the redistribution of Fe in the Al_2O_3 films and the near-surface regions of the Si substrate via secondary ion mass spectrometry (SIMS) analysis.

The samples used in this work were boron-doped p-type float-zone (FZ) silicon wafers with known doses of intentional iron contamination, introduced by implanting the Si wafers with ^{56}Fe using a relatively low ion implantation energy of 70 keV. The implantation doses were 1.8×10^{11} cm^{-2} and 1.8×10^{12} cm^{-2} for the wafers with a resistivity of 0.9 Ω cm

and a thickness of 180 μm (after saw damage etching in an alkaline solution), which corresponded to volumetric Fe concentrations of 10^{13} cm^{-3} and 10^{14} cm^{-3}, respectively. 270-μm thick and 1.7 Ω cm p-type FZ-Si wafers were also used, which were implanted with 8×10^{10} cm^{-2} Fe to result in a volumetric Fe concentration of 3×10^{12} cm^{-3}. After ion implantation, the wafers were annealed at 1000 °C to uniformly distribute the implanted Fe throughout the wafer thickness. The implantation energy and doses used here, combined with a 1000 °C post-implantation anneal, are expected to result in negligible residual damage in silicon wafers.[12]

At 1000 °C, the Fe solubility in Si is 4×10^{14} cm^{-3},[13] above the targeted Fe concentrations of 3×10^{12}–10^{14} cm^{-3}. The Fe implanted samples, together with non-implanted FZ-Si control wafers, were RCA cleaned and loaded into a furnace at 700 °C, ramped up in dry oxygen at 10 °C/min, annealed at 1000 °C in dry oxygen for 1.5 h, followed by 0.5 h in nitrogen, before being cooled down in nitrogen at a rate of 10 °C/min, and unloaded at 800 °C. After unloading, the wafers were left to cool in a high airflow and reached room temperature within minutes. The 1000 °C distribution anneal also resulted in thermally grown silicon dioxide (SiO_2) layers around 110 nm thick on the wafer surfaces, which not only acted as diffusion barriers for any possible furnace contaminants but also provided sufficient surface passivation for samples which were set aside as the silicon dioxide (SiO_2) controls.

A sub-set of the samples had the SiO_2 layers removed in a dilute HF (1%) solution and then received a chemical etch in a HNO_3:HF (10:1) solution, which further reduced the wafer thicknesses from 180 μm to 160–165 μm and from 270 μm to 260–265 μm. These wafers were then coated with plasma-assisted (PA) ALD Al_2O_3 films on both sides, using a Beneq TFS-200 ALD system, at a deposition temperature of 175 °C, with a deposition rate of around 0.1 nm/cycle. Films of 20, 40, and 80 nm thick were deposited. Trimethylaluminum (TMA) was used as the precursor in ALD, and PA-ALD used as an oxygen plasma as the oxidant.

To assess the Fe_i loss kinetics in the silicon bulk, both the ALD Al_2O_3 and thermally grown SiO_2 coated Fe-implanted samples were annealed on a hotplate in air for cumulative times at 425 °C. Non-implanted FZ-Si wafers with either SiO_2 or Al_2O_3 coatings, which were co-processed in the proceeding steps, were co-annealed at 425 °C to monitor any changes in surface passivation. The Fe-implanted wafers were pseudosquares of $4 \, cm \times 4 \, cm$, and the co-processed controls were quarters of 10-cm diameter circular wafers. After each cumulative anneal step, a WCT-120 tool from Sinton Instruments[14] was used to measure the effective minority carrier lifetime of the samples. The interstitial Fe concentration ($[Fe_i]$) in the silicon bulk was determined from lifetimes measured in the isolated Fe_i and FeB pair states,[9,10] with strong illumination used to dissociate the FeB pairs.[15] A photographic flasher provided strong white light with a peak intensity of several hundred suns and a flash time of 1/300 s. The flashes were repeated 20–30 times until lifetime saturation, ensuring a full dissociation of the FeB pairs.

The redistribution of Fe after annealing was measured by SIMS depth profiling of the Fe concentration in the annealed Al_2O_3 or SiO_2 layer and the underlying Si substrate. SIMS measurements were conducted at EAG Laboratories. The nominal depth resolution was better than 1.5 nm/step although the actual resolution was limited by the mixing of bombarded ions during SIMS measurements. Silicon and aluminium were monitored as marker species with the secondary ion intensity qualitatively measured, which served to distinguish the locations of the Al_2O_3 or SiO_2 surface layers, and the Si wafer bulk, in the depth profiles. Descriptions of the samples for SIMS measurements are given in Table I.

The last two samples in Table I were processed in our previous work, where most of the experimental details can be found.[7] These 20-nm thick SiO_2 layers were grown from annealing wafers at 900 °C for 1 h in dry oxygen, followed by 1 h in nitrogen, before being cooled in nitrogen at a rate of 10 °C/min and unloaded at 750 °C. The SIMS results for these two samples were not shown in Ref. 7.

Note that an 80-nm thick ALD Al_2O_3 film is not typically used in silicon solar cells. This thickness was chosen here because SIMS analysis is prone to measurement artefact extending tens of nanometres from the wafer surfaces, which gives an apparent increase in the Fe concentration towards the surfaces. To ensure that the SIMS measurements of the

80-nm Al_2O_3 samples are representative of the gettering behaviours of typical ALD Al_2O_3 films (commonly less than 30 nm), the Fe_i loss kinetics of samples coated with Al_2O_3 films of different thicknesses were measured and compared, as shown in Fig. 1.

The effective lifetime measured on non-implanted FZ-Si control samples was largely limited by surface recombination and was found to be always 1–3 orders of magnitude higher than the lifetime of the Fe-contaminated samples, indicating the dominance of bulk lifetime. The lifetime of the control samples was also found to be stable under the strong illumination used to break FeB pairs for $[Fe_i]$ measurements. The extraction of $[Fe_i]$ from effective lifetime measurements was therefore not affected by the changes in surface passivation during illumination or during annealing.

As shown in Fig. 1, the ALD Al_2O_3 and the thermal SiO_2 samples display very different Fe_i loss kinetics. The Al_2O_3 samples, despite different film thicknesses and initial Fe_i concentrations, all show an initial fast Fe_i loss, which can be fitted by a diffusion-limited surface gettering model with apparent Fe diffusivities of $7 \times 10^{-9} \, cm^2/s$ and $5 \times 10^{-9} \, cm^2/s$. This model takes into account the wafer thickness and simulates the changes in the bulk impurity concentration for impurities that diffuse into the gettering sites on both sides of the wafer surfaces, with a fitted apparent impurity diffusivity.[16] Although the experimental data for the $3 \times 10^{12} \, cm^{-3}$ sample demonstrate a much slower decline in $[Fe_i]$ compared to the rest of the Al_2O_3 samples, the measured kinetics can be fitted

TABLE I. Samples for SIMS analysis.

| Surface layers	Initial bulk [Fe_i]	Annealing temperature and time
ALD Al_2O_3 80 nm	$10^{14} \, cm^{-3}$	425 °C, 1.8 h (short anneal)
ALD Al_2O_3 80 nm	$10^{14} \, cm^{-3}$	425 °C, 18 h (long anneal)
ALD Al_2O_3 80 nm	$3 \times 10^{12} \, cm^{-3}$	425 °C, 18 h
ALD Al_2O_3 80 nm	Nil – No Fe implantation	425 °C, 18 h
Thermally grown SiO_2 110 nm	$10^{13} \, cm^{-3}$	425 °C, 18 h
Thermally grown SiO_2 20 nm	$10^{13} \, cm^{-3}$	700 °C, 0.5 h
Thermally grown SiO_2 20 nm	Nil – No Fe implantation	700 °C, 0.5 h
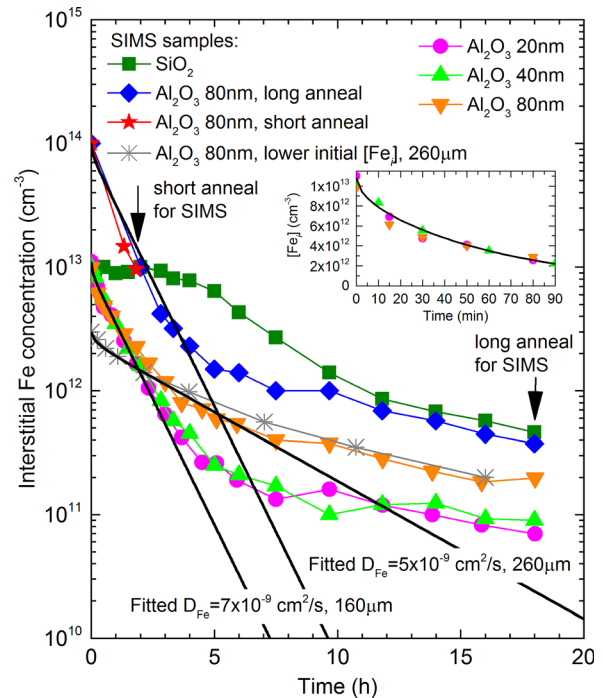
FIG. 1. Fe_i loss kinetics in Fe-contaminated silicon wafers coated with ALD Al_2O_3 films of different thicknesses, or with thermally grown SiO_2 layers, cumulatively annealed at 425 °C. The straight lines are fits to the experimental data using a diffusion-limited surface-loss model, yielding fitted apparent Fe diffusivities.[16] Lines connecting the symbols are guides to the eye. The inset shows the Fe_i kinetics during the initial short anneals, for the Al_2O_3 samples with an initial $[Fe_i]$ of $10^{13} \, cm^{-3}$. Note that $[Fe_i]$ in the inset is plotted on a linear scale instead of a logarithmic scale, and time is in the unit of minutes instead of hours. The SIMS samples have the corresponding SIMS data shown in Figs. 2 (Al_2O_3 samples) and 3 (SiO_2 sample).

by a similar apparent Fe diffusivity, indicating that the slower [Fe$_i$] reduction is largely caused by different wafer thicknesses. The reported Fe diffusivity in the literature is 1.5×10^{-8} cm^2/s at $425\,°$C,[13] which is close to the fitted apparent Fe diffusivities in Fig. 1, suggesting that this fast initial Fe$_i$ loss stage can be considered as representing the diffusion-limited loss of interstitial iron to the surfaces.

The inset in Fig. 1 shows a plot of the fast Fe$_i$ loss kinetics, on a time scale that is relevant for the activation of ALD Al$_2$O$_3$ films. As shown in the inset of Fig. 1, for a typical 160-μm wafer, a 10-min anneal at $425\,°$C reduces 20% of the bulk Fe$_i$ concentration, and a 30-min anneal reduces the Fe$_i$ concentration by half. Iron has a moderate diffusivity in silicon. This reported gettering effect should be taken into consideration in studies that use ALD Al$_2$O$_3$ films as surface passivation coatings, to avoid misinterpretation.

The initial fast Fe$_i$ reduction stage of the Al$_2$O$_3$ samples is then followed by a slow-down of the rate of Fe$_i$ loss, with the thicker 80-nm films demonstrating an earlier onset of the slow-down. It is worth mentioning that we also measured the Fe$_i$ loss kinetics in thermal H$_2$O-based ALD Al$_2$O$_3$ coated silicon wafers, which were deposited using the same ALD system at $200\,°$C, and similar, reproducible Fe$_i$ loss kinetics were observed.

The SiO$_2$ coated sample, on the other hand, first shows little change in the Fe$_i$ concentration. With increasing annealing time, however, the [Fe$_i$] reduction is initiated and then accelerates, with the onset occurring after 3–5 h. For longer times, both the SiO$_2$ and Al$_2$O$_3$ samples show a similar rate of Fe$_i$ loss.

To understand the observed gettering effects in Fig. 1, SIMS analysis was performed on the cumulatively annealed Al$_2$O$_3$ (Fig. 2) and SiO$_2$ (Fig. 3) samples to reveal Fe redistribution. SIMS detects the total Fe concentration regardless of the electrical state, i.e., it detects both dissolved and precipitated Fe. Note that all the SIMS Fe profiles in Figs. 2 and 3, as well as in our previous work,[7] demonstrate a near-surface Fe increase, for samples with different coatings and with or without previous bulk Fe contamination. This suggests that the near-surface Fe increase does not arise from the gettering of Fe from the silicon bulk and is likely a measurement artefact in SIMS analysis, possibly caused by unintentional surface contamination during handling. Moreover, the diffusion length of Fe in thermal SiO$_2$ during a $425\,°$C 18-h anneal, from extrapolating the diffusivity data,[17] is estimated to be less than 2 nm, which shows the unlikelihood of Fe to diffuse through an 110-nm thick SiO$_2$ layer to reach the surface.

Figure 2 shows that, for samples previously contaminated with Fe$_i$ in the silicon bulk, high Fe concentration peaks are observed at the Al$_2$O$_3$/Si interfaces, with higher initial bulk [Fe$_i$] demonstrating higher Fe peaks. The shifts in the peak position along the depth profiles (i.e., x-axis) originate from the slight variations in the deposited film thicknesses, as reflected by the qualitative measurements of the Si and Al matrixes (upper curves in Fig. 2). On the other hand, the Al$_2$O$_3$ control sample without prior bulk Fe$_i$ contamination displays no such Fe peak, which clearly indicates that the observed Fe peaks at the Al$_2$O$_3$/Si interfaces arise from Fe$_i$ previously distributed in the silicon wafer bulk; in

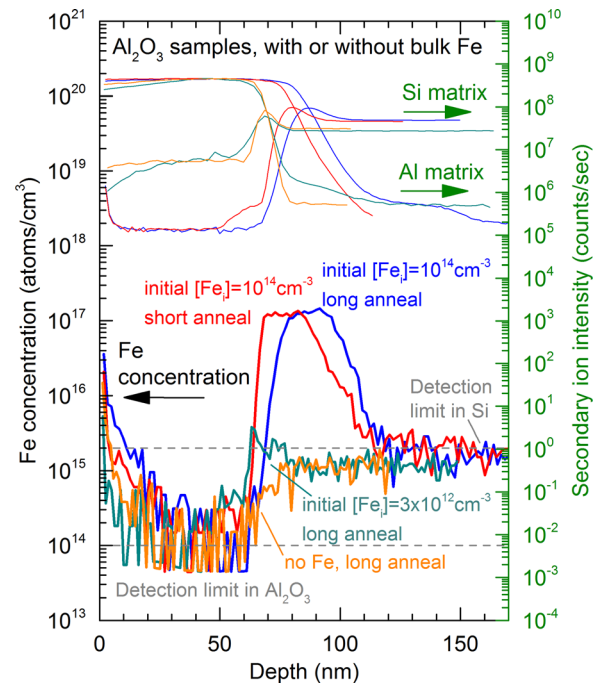other words, Fe$_i$ is gettered from the silicon bulk to the Al$_2$O$_3$/Si interface. Quantitatively, for samples initially contaminated with 10^{14} cm^{-3} bulk [Fe$_i$] and with the same Al$_2$O$_3$ films deposited on both sides of the wafer surfaces, the integrated SIMS Fe concentration in these interface peaks is about half of the known implanted Fe dose. Given that the ion yield from Al$_2$O$_3$ may depend on the film deposition
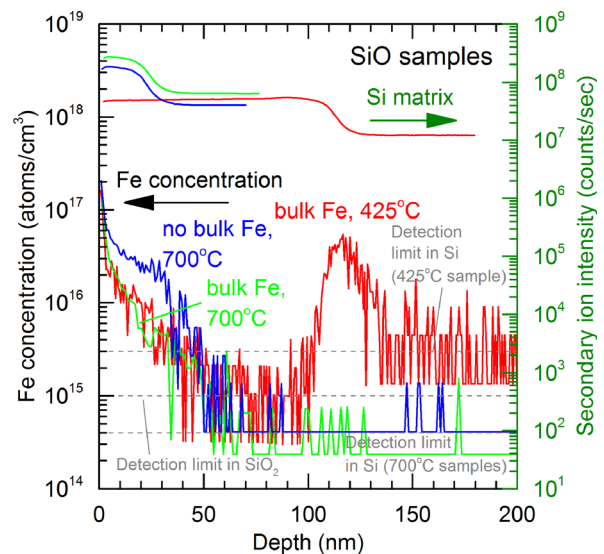

FIG. 2. SIMS profiles of the Fe distribution in ALD Al$_2$O$_3$ coated silicon wafers cumulatively annealed at $425\,°$C. The samples had different initial bulk Fe concentrations and were annealed for either short (1.8 h) or long (18 h) time durations. The upper curves are a qualitative measure of the Al and Si matrixes (plotted against the y-axis on the right), which are used to indicate the positions of the Al$_2$O$_3$ films and the Si bulk in the depth profiles. The detection limits of Fe in Al$_2$O$_3$ and in Si are marked by dashed lines.

FIG. 3. SIMS profiles of the Fe distribution in thermally grown SiO$_2$ coated silicon wafers, annealed at either $425\,°$C for a total of 18 h, with an initial bulk [Fe$_i$] of 10^{13} cm^{-3}, or annealed at $700\,°$C for 30 min, with or without previous 10^{13} cm^{-3} bulk Fe$_i$. The top curves are used to indicate the position of the SiO$_2$ layer and the Si bulk in the depth profiles. The detection limits of Fe in SiO$_2$ and in Si are marked by dashed lines.

conditions, this discrepancy in the Fe concentration is considered reasonable and confirms that the Fe peaks in SIMS profiles originate from the implanted Fe previously distributed in the silicon bulk.

The accumulation of Fe at the SiO_2/Si interface is observed for the Fe-contaminated SiO_2 sample annealed at $425\,°C$, as shown in Fig. 3. The quantitative Fe concentration of this interface peak is again found to be about half of the known implanted Fe dose, showing general agreement with the reduced $[Fe_i]$ in the silicon wafer bulk measured by QSSPC. The $700\,°C$ 30-min annealed Fe-contaminated SiO_2 sample, however, shows little change in bulk $[Fe_i]$ from QSSPC measurements, consistent with previous results,[7] and the sample also demonstrates no Fe peak at the SiO_2/Si interface. The solubility of Fe at $425\,°C$ is in the range of $10^5\,cm^{-3}$ (Ref. 13) to $10^8\,cm^{-3}$ (from extrapolation[18]), and the solubility at $700\,°C$ is $(1–6) \times 10^{11}\,cm^{-3}$.[13,18] It is well known that Fe-silicide precipitates tend to form at the SiO_2/Si interfaces (see, for example, Ref. 11 for a review). The observed Fe peak at the SiO_2/Si interface for the $425\,°C$ 18-h annealed sample is therefore likely due to Fe precipitation. The lack of Fe precipitates for the $700\,°C$ 30-min annealed sample may relate to the short annealing time, as Fig. 1 shows that the onset of Fe_i reduction for SiO_2 coated FZ-Si wafers requires some time.

Fe precipitation at the SiO_2/Si interface could well explain the observed Fe_i loss kinetics for the SiO_2 sample shown in Fig. 1. The thermal SiO_2/Si interface may require a certain nucleation time for the formation of precipitation sites, and hence, the SiO_2 sample showed little change in $[Fe_i]$ in the early stages. These developing precipitation sites later facilitate Fe precipitation, and therefore, a faster $[Fe_i]$ loss is observed for the SiO_2 sample in later stages.

The underlying mechanism for the observed Fe peaks at the Al_2O_3/Si interfaces (Fig. 2), however, remains unknown at this stage. As a thin silicon oxide (SiO_x) layer is known to reside at the ALD Al_2O_3/Si interface,[19] this Fe peak may be caused by Fe precipitation at the SiO_x/Si interface, similar to Fe precipitation at the thermal SiO_2/Si interface.[11] However, Fig. 1 shows that the ALD Al_2O_3 and thermal SiO_2 samples have very different Fe_i loss kinetics. Hence, Fe accumulation at the ALD Al_2O_3/Si interface could be caused by a different mechanism, for example, by impurity segregation at the Al_2O_3/Si interface. Further temperature-dependent gettering studies will be required to assess the hypotheses.

The 2-stage Fe_i loss kinetics of the Al_2O_3 samples (Fig. 1) is investigated by conducting SIMS analysis on samples undergoing either short (1.8 h) or long (18 h) anneals (Fig. 2). As shown in Fig. 1, the short anneal sample was still in the initial fast Fe_i loss stage, whereas the long anneal sample had experienced both fast and slow Fe_i reductions. The remaining $10^{13}\,cm^{-3}$ Fe_i gettered by the long anneal sample, if gettered to the 80-nm Al_2O_3 film, would demonstrate an Fe concentration of $10^{16}\,cm^{-3}$ distributed in the film, similar to the SIMS Fe profiles of PECVD SiN_x samples.[7] If the remaining $10^{13}\,cm^{-3}$ Fe_i were gettered to the Al_2O_3/Si interface, where Fe peaks are shown be ~20 nm wide, the long anneal sample would demonstrate a $4 \times 10^{16}\,cm^{-3}$ increase in the peak height, which would be hardly discernible from the existing Fe peak from a short anneal (Fig. 2). The SIMS

results in Fig. 2 show that the initial fast Fe_i loss is caused by Fe accumulation at the Al_2O_3/Si interface, and the second slow reduction stage is not due to Fe segregation into the Al_2O_3 film. The slow reduction may arise from Fe accumulation at the Al_2O_3/Si interface or Fe gettering by bulk defects within the FZ-Si wafers. As shown in Fig. 1, the onset of the slow reduction stage seems to relate to the film thickness, which may depend on the film properties.[19] Further studies are needed to understand this correlation.

It is interesting to note that although both ALD Al_2O_3 and PECVD SiN_x films display similar diffusion-limited gettering kinetics at around $400\,°C$, ALD Al_2O_3 films rely on the Al_2O_3/Si interfaces to achieve impurity accumulation, while PECVD SiN_x films relocate the impurities into the bulk of the films themselves.[7]

The reported gettering effect of ALD Al_2O_3 films is beneficial for improving the bulk silicon material quality, which can be conveniently coupled with the necessary passivation activation anneal. Further temperature-dependent gettering studies, combined with a close monitoring of the surface passivation quality, will be useful for assessing the overall effect of annealing at different temperatures and times. The potential impact of impurity accumulation on device performance, for example, in terms of shunting, requires further investigations.

In summary, this letter presents experimental evidence for the gettering effect of ALD Al_2O_3 films at a typical film activation temperature of $425\,°C$, by examining the concentration and re-distribution of iron in silicon. The gettering process is found to be largely diffusion-limited in the early stages, meaning that during a typical 30-min $425\,°C$ passivation activation anneal, the dissolved Fe in a 160-μm thick silicon wafer is reduced by half. The gettering effect is shown to be caused by the aggregation of iron at the ALD Al_2O_3/Si interface.

[1]B. Hoex, J. Schmidt, R. Bock, P. P. Altermatt, M. C. M. van de Sanden, and W. M. M. Kessels, "Excellent passivation of highly doped p-type Si surfaces by the negative-charge-dielectric Al_2O_3," Appl. Phys. Lett. **91**, 112107 (2007).

[2]B. Hoex, J. J. H. Gielis, M. C. M. van de Sanden, and W. M. M. Kessels, "On the c-Si surface passivation mechanism by the negative-charge-dielectric Al_2O_3," J. Appl. Phys. **104**, 113703 (2008).

[3]W. Liang, K. J. Weber, D. Suh, S. P. Phang, J. Yu, A. K. McAuley et al., "Surface passivation of boron-diffused p-type silicon surfaces with (1 0 0) and (1 1 1) orientations by ALD Al_2O_3 layers," IEEE J. Photovoltaics **3**, 678–683 (2013).

[4]G. Dingemans and W. M. M. Kessels, "Status and prospects of Al_2O_3-based surface passivation schemes for silicon solar cells," J. Vac. Sci. Technol., A **30**, 040802 (2012).

[5]A. Richter, S. Henneck, J. Benick, M. Hörteis, M. Hermle, and S. Glunz, "Firing stable Al_2O_3/SiN_x layer stack passivation for the front side boron emitter of n-type silicon solar cells," in Proceedings of the 25th European Photovoltaic Solar Energy Conference and Exhibition (2010), pp. 1453–1456.

[6]S. Gatz, H. Hannebauer, R. Hesse, F. Werner, A. Schmidt, T. Dullweber et al., "19.4%-efficient large-area fully screen-printed silicon solar cells," Phys. Status Solidi RRL **5**, 147–149 (2011).

[7]A. Y. Liu, C. Sun, V. P. Markevich, A. R. Peaker, J. D. Murphy, and D. Macdonald, "Gettering of interstitial iron in silicon by plasma-enhanced chemical vapour deposited silicon nitride films," J. Appl. Phys. **120**, 193103 (2016).

[8]G. Dingemans, F. Einsele, W. Beyer, M. C. M. van de Sanden, and W. M. M. Kessels, "Influence of annealing and Al_2O_3 properties on the hydrogen-induced passivation of the Si/SiO_2 interface," J. Appl. Phys. **111**, 093713 (2012).

[9]G. Zoth and W. Bergholz, "A fast, preparation-free method to detect iron in silicon," J. Appl. Phys. **67**, 6764–6771 (1990).

[10]D. H. Macdonald, L. J. Geerligs, and A. Azzizi, "Iron detection in crystalline silicon by carrier lifetime measurements for arbitrary injection and doping," J. Appl. Phys. **95**, 1021–1028 (2004).

[11]A. A. Istratov, H. Hieslmair, and E. R. Weber, "Iron contamination in silicon technology," Appl. Phys. A **70**, 489–534 (2000).

[12]D. Macdonald, P. N. K. Deenapanray, and S. Diez, "Onset of implant-related recombination in self-ion implanted and annealed crystalline silicon," J. Appl. Phys. **96**, 3687–3691 (2004).

[13]A. A. Istratov, H. Hieslmair, and E. R. Weber, "Iron and its complexes in silicon," Appl. Phys. A **69**, 13–44 (1999).

[14]R. A. Sinton and A. Cuevas, "Contactless determination of current–voltage characteristics and minority-carrier lifetimes in semiconductors from quasi-steady-state photoconductance data," Appl. Phys. Lett. **69**, 2510–2512 (1996).

[15]L. Geerligs and D. Macdonald, "Dynamics of light-induced FeB pair dissociation in crystalline silicon," Appl. Phys. Lett. **85**, 5227 (2004).

[16]J. D. Murphy and R. J. Falster, "The relaxation behaviour of supersaturated iron in single-crystal silicon at 500 to 750 °C," J. Appl. Phys. **112**, 113506 (2012).

[17]D. A. Ramappa and W. B. Henley, "Diffusion of iron in silicon dioxide," J. Electrochem. Soc. **146**, 3773–3777 (1999).

[18]J. D. Murphy and R. J. Falster, "Contamination of silicon by iron at temperatures below 800 °C," Phys. Status Solidi RRL **5**, 370–372 (2011).

[19]F. Werner, B. Veith, D. Zielke, L. Kühnemund, C. Tegenkamp, M. Seibt *et al.*, "Electronic and chemical properties of the c-Si/Al_2O_3 interface," J. Appl. Phys. **109**, 113701 (2011).